Surface phase transitions: Roughening, preroughening, orientational roughening, and reconstruction in an isotropic frustrated Ising model

B. Kahng
Department of Chemistry, University of California, Berkeley, California 94720

A. Berera
Department of Physics, University of California, Berkeley, California 94720

K. A. Dawson
Department of Chemistry, University of California, Berkeley, California 94720
(Received 23 July 1990)

We study the roughening, the preroughening, and the orientational roughening transitions for interfaces between phases in the isotropic competing Ising Hamiltonian $\mathcal{H}=-J\sum_{\mathrm{NN}}s_is_j-2M\sum_{\mathrm{DNN}}s_is_j-M\sum_{\mathrm{LNNN}}s_is_j$. The symbols, NN, DNN, and LNNN represent nearest-neighbor, diagonal-nearest-neighbor, and linear-next-nearest-neighbor pairs, respectively, with $J>0$ and $-\infty<M<\infty$. By performing low-temperature expansions in the three-dimensional cubic lattice, it is found that the roughening transition curve passes through the region in which paramagnetic, ferromagnetic, and modulated phases merge, and is parallel to the phase boundary of ferromagnetic and modulated phases. It is also found that crossover behavior occurs in the roughening transition from the surface tension dominant regime to the bending-energy dominant regime. We examine the preroughening transition for the case of the restricted solid-on-solid (RSOS) model. The preroughening transition line is found to be distinct from the roughening transition line. This confirms the recent prediction by den Nijs [Phys. Rev. Lett. **64**, 435 (1990)]. Within the RSOS model, we find a multistate point for reconstructed surface structures. This is analogous to the multistate point in the bulk phase diagram. The orientational roughening transition is also examined. However, it was not possible to obtain the orientational roughening transition line at a temperature higher than that of the translational roughening transition, presumably due to the limited order of the low-temperature series. The results deduced from the low-temperature expansions are compared to the sine-Gordon renormalization-group calculations based on the SOS and RSOS models. Finally we discuss the implications of the surface structure, and the connections with bulk structure.

I. INTRODUCTION

The interface between crystals and vacuums or between solids and fluids has been thoroughly studied in recent years. There is also considerable technological interest in surface magnetic structure. The model we shall study has implications for a number of such phenomena. In particular, we shall examine the roughening transition and the equilibrium surface or interface structure of a spin model with extended interactions. Recall that the roughening transition[1] for the nearest-neighbor Ising model interface occurs at a temperature lower than the Curie temperature and belongs to a different universality class,[2,3] the Kosterlitz-Thouless transition, than that of the bulk phase. However, the roughening transition for more complicated Hamiltonians is not so well understood, though one might expect to have more extended interactions than nearest neighbors at the surfaces of many materials.

We consider the Ising Hamiltonian with interactions

$$\mathcal{H}=-J\sum_{\langle i,j\rangle}^{\mathrm{NN}}S_iS_j-\gamma M\sum_{\langle i,j\rangle}^{\mathrm{DNN}}S_iS_j-M\sum_{\langle i,j\rangle}^{\mathrm{LNNN}}S_iS_j\ , \qquad (1.1)$$

where NN, DNN, LNNN mean, respectively, nearest-neighbor, diagonal-nearest-neighbor, and linear-next-nearest-neighbor pairs on a simple cubic lattice. We consider the case $J>0$ and $-\infty<M<\infty$. The choice of $\gamma=2$ for the DNN interactions generates the richest bulk phase diagram.[4,5] Therefore we will consider this case for the surface Hamiltonian in this paper. The Hamiltonian Eq. (1.1) exhibits many interesting phases as a consequence of the competing interactions in the region $J>0$, $M<0$. It was originally introduced in a study of microemulsion,[4-8] but may also be applied to a number of physical systems such as binary alloys and ferrimagnets.[9] It is worth noting that the couplings are spatially isotropic, so that for some systems the Hamiltonian is more realistic than traditional anisotropic models. Moreover it possesses a richer phase diagram than that of the axial-next-nearest-neighbor Hamiltonian[10] (ANNNI).

The competing interactions in the spin Hamiltonian generate many modulated phases, as well as the ferromagnetic and paramagnetic phases. Within mean-field theory the bulk phase diagram of this Hamiltonian has an isotropic Lifshitz point $\mathcal{L}$ at which the paramagnetic, fer-

romagnetic, and infinite period lamellar phases merge. Naive dimensional arguments indicate that the lower critical dimension for the Lifshitz point $\mathcal{L}$ should be $d_L=4$, so the mean-field theory is unlikely to be valid in this region.[11,12] However, if the layers are sufficiently far apart, then one might argue that the disordering transition is driven by a roughening phenomenon. As we shall see, the curve of roughening transition, as derived from low-temperature expansion, does indeed pass through the point $\mathcal{L}$ as determined by simulations.

In this paper we investigate the property of the interface in relation to the bulk phase structure. Our study relies mainly on the results of low-temperature series expansions. The outline of the paper is as follows. In Sec. II the roughening transition is considered. First, in Sec. II A, we present a computer algorithm to enumerate clusters and fugacities of overtuned spins at low temeprature. We also introduce modified order parameters, which are more appropriate for the roughening transition of the Hamiltonian (1.1). In Sec. II B we present the solid-on-solid model (SOS) and the restricted solid-on-solid model (RSOS) associated with the Hamiltonian (1.1). In Sec. II A we present the roughening transition line in the parameter space of $j\equiv J/kT$ and $m\equiv M/kT$, obtained from the low-temperature expansion and Padé analysis. We find the crossover behavior from the surface tension dominant regime to the bending-energy dominant regime, and discuss this crossover behavior in momentum space.

In Sec. III the preroughening transition is considered. In Sec. III A we present the preroughening transition line obtained from the low-temperature series. In Sec. III B we study the reconstructed surface structures and their connection to the multistate point in the bulk phase diagram. In Sec. IV the orientational roughening transition is considered. The final section is devoted to the discussions and conclusions. In Sec. V A we briefly review the sine-Gordon renormalization-group (RG) study for the roughening and preroughening transitions; the latter was first discussed by den Nijs. We also discuss the sine-Gordon RG study for the orientational roughening and translational roughening transitions. In Sec. V B we discuss the connections of bulk structure to surface structure.

II. ROUGHENING TRANSITION

A. Low-temperature expansion

To obtain the roughening transition line in the parameter space of $j=J/kT$ and $m=M/kT$, we shall apply the method of low-temperature series expansion. Indeed this method was applied in one of the first studies of the roughening transition for the nearest-neighbor model.[2] Our treatment is quite similar in spirit, but with the Hamiltonian defined in Eq. (1.1). In general the task of constructing the low-temperature series for the surface transition is more demanding than for the bulk case because the contributions due to the excluded volume of the disconnected clusters depend on the relative heights of the disconnected clusters.

We begin this section by outlining the system we shall study. First, we define a three-dimensional cubic lattice of linear dimensions L with periodic-boundary conditions in the x and y directions and antiperiodic boundary conditions between the positive- and the negative-z boundaries. The interface at $T=0$ is chosen to lie at $z=0$ and in the zero temperature state, all spins are positive for $z<0$ and negative for $z>0$. Thus the ground-state normalized layer density is $\rho(z)=1$ for $z<0$, associated with positive spins, and $\rho(z)=0$ for $z>0$, associated with negative spins. Spins are located at positions on half-integer layers, $z=\pm\frac{1}{2},\pm\frac{3}{2},\ldots,\pm L/2$.

To study the excitations above the ground state, we generate clusters of overtuned spins by a computer algorithm that is based on Martin's backtracking method.[13] For each cluster, we then calculate the energy and the associated change in height with respect to the flat surface. The present problem of generating clusters is considerably more complicated than for the Ising case, because one must consider the interaction energy of clusters that are separated by DNN or by LNNN sites. These are considered to be connected clusters for the Hamiltonian, Eq. (1.1), whereas they are disconnected for the Ising Hamiltonian. The principal idea we have used in overcoming this problem is that the DNN and LNNN sites are considered to have higher values than their physical coordination numbers. Accordingly, the total coordination number of the system is 24 instead of 6 as for the cubic lattice. The enlarged coordination number requires significantly more computer time. We have also developed a computer program to consider completely disconnected clusters, leaving only a relatively small number to do by hand. The main problem in computing contributions due to disconnected clusters is counting the excluded volume, which depends on the relative heights. Therefore, whenever clusters are generated or deleted, we count the number of NN, DNN, and LNNN sites of the occupied sites for each height. This method is analogous to the one used to count the perimeter sites of percolation clusters.[14]

To study the roughening transition, Weeks *et al.*[2] introduced two types of order parameter, moments of the density gradient and the surface density. First, the moments of the density gradient are defined as

$$\langle z^{2n}\rangle=\sum_{z=-\infty}^{\infty}[\rho(z-\tfrac{1}{2})-\rho(z+\tfrac{1}{2})]z^{2n}\ , \tag{2.1}$$

which diverges as $T\to T_R$. Another order parameter is defined via the surface density; thus

$$\mathcal{R}=\frac{1}{1-2\rho(\frac{1}{2})}\ , \tag{2.2}$$

which again diverges as $T\to T_R$ because the surface density $\rho(\frac{1}{2})$ approaches the value of one-half as $T\to T_R$. However, since the Hamiltonian, Eq. (1.1), contains the LNNN interaction, it is more natural to define the quantity

$$\mathcal{R}'=\frac{1}{1-\rho(\frac{1}{2})-\rho(\frac{3}{2})}\ , \tag{2.3}$$

which also diverges, since $\rho(\frac{1}{2})+\rho(\frac{3}{2})$ approaches unity

as $T \to T_R$. This order parameter includes the bulk excitation at $z=\frac{3}{2}$, which is regarded as a connected cluster by the LNNN interaction with the flat surface.

We obtain the low-temperature series of the order parameters, $\langle z^2 \rangle$ and $\mathcal{R}'$, in terms of the small parameters $x \equiv e^{-4M/kT}$ and $y \equiv e^{-4J/kT}$. We consider the case of $J > M$ including the region of the competing interaction. In this region, y is smaller than x, so that one may take y as a small parameter of the series expansion. Thus the low-temperature series may be written

$$\langle z^2 \rangle_{\mathrm{BO}} = \sum_{p=0}^{\infty} \left[\sum_{q=0}^{\infty} A_{\mathrm{BO}}(p,q) x^q \right] y^p , \tag{2.4}$$

$$\mathcal{R}'_{\mathrm{BO}} = \sum_{p=0}^{\infty} \left[\sum_{q=0}^{\infty} B_{\mathrm{BO}}(p,q) x^q \right] y^p , \tag{2.5}$$

where the subscript BO means that the series includes bulk excitations and overhangs. Later in this paper we shall use the same notation to distinguish this series from the ones based on the SOS and the RSOS models. The series for $\langle z^2 \rangle_{\mathrm{BO}}$ and $[\rho(\frac{1}{2})+\rho(\frac{3}{2})]_{\mathrm{BO}}$ are derived up to $O(y^7)$, and the polynomials are given in the Appendix, Eqs. (A1) and (A2). We note that the coefficients reduce to the nearest-neighbor Ising ones in the limit of $x \to 1$, that is, as $M \to 0$. The roughening transition singularity is determined by using the standard d log Padé approximant analysis. Since the series is obtained up to order $O(y^7)$, we use only the [2,2] d log Padé analysis. In order to perform these calculations, one may first choose x values, and then locate the singular values, $y_R(x)$, for a given x value. The dominant singularity is assumed to be of the form

$$\sim y^2 (y - y_R)^{-\theta} . \tag{2.6}$$

Also, according to the sine-Gordon formalism,[15] the singularity for the interfacial width is related to the correlation length ξ by

$$\langle z^2 \rangle \sim \ln \xi \sim |T - T_R|^{-\nu} . \tag{2.7}$$

Although the d log Padé analysis is performed only to order [2,2] we believe the analysis is sufficient to derive an accurate phase diagram of the roughening transition. The corrections due to the higher-order d log Padé terms are presumably of comparable magnitude to those for the nearest-neighbor model, and in this case the [2,2] approximation is typically accurate to 5%.

As an additional check on this conclusion we have carried out the following analysis. The location of the singularity and its residue are first fixed according to the [2,2] Padé analysis. This implies an infinite series, the leading terms of which agree with the low-temperature analysis. Now one can begin to vary the coefficients in this series beyond those that we explicitly determined in the low-temperature expansion. It is found that variation in the coefficients of the $O(y^2)$ and higher-order terms have almost no effect on the properties we have calculated. It therefore seems unlikely that correct treatment of such terms within the low-temperature analysis can affect our results.

B. The SOS model and the RSOS model

We now consider the solid-on-solid model in which bulk excitations and overhangs are excluded, and the restricted solid-on-solid model, which is an SOS-type model where the differences between NN heights are restricted to $\delta h = 0, \pm 1$. The SOS Hamiltonian that is equivalent to Eq. (1.1) is

$$\mathcal{H}_{\mathrm{SOS}} = (J+4M) \sum_{\langle r,r' \rangle}^{\mathrm{NN}} |h_r - h_{r'}| + 2M \sum_{\langle r,r' \rangle}^{\mathrm{DNN}} |h_r - h_{r'}| + M \sum_{\langle r,r' \rangle}^{\mathrm{LNNN}} |h_r - h_{r'}| , \tag{2.8}$$

while the RSOS Hamiltonian is

$$\mathcal{H}_{\mathrm{RSOS}} = J \sum_{\langle r,r' \rangle}^{\mathrm{NN}} |h_r - h_{r'}| + 2M \sum_{\langle r,r' \rangle}^{\mathrm{DNN}} |h_r - h_{r'}| + M \sum_{\langle r,r' \rangle}^{\mathrm{LNNN}} |h_r - h_{r'}| , \tag{2.9}$$

where NN, DNN, and LNNN mean nearest-neighbor columns, diagonal-nearest-neighbor columns, and linearly next-nearest-neighbor columns, respectively. The corresponding Gaussian Hamiltonians are

$$\mathcal{H}_{\mathrm{SOS}} = (J+4M) \sum_{\langle r,r' \rangle}^{\mathrm{NN}} (h_r - h_{r'})^2 + 2M \sum_{\langle r,r' \rangle}^{\mathrm{DNN}} (h_r - h_{r'})^2 + M \sum_{\langle r,r' \rangle}^{\mathrm{LNNN}} (h_r - h_{r'})^2 , \tag{2.10}$$

$$\mathcal{H}_{\mathrm{RSOS}} = J \sum_{\langle r,r' \rangle}^{\mathrm{NN}} (h_r - h_{r'})^2 + 2M \sum_{\langle r,r' \rangle}^{\mathrm{DNN}} (h_r - h_{r'})^2 + M \sum_{\langle r,r' \rangle}^{\mathrm{LNNN}} (h_r - h_{r'})^2 . \tag{2.11}$$

We note that the coupling constants between the NN columns are slightly different in the SOS model and the RSOS model. This is a reflection of the difference in the number of DNN sites within the NN columns.

For the SOS and RSOS models, we have also obtained the series for the second moment of height in a low-temperature expansion. These are defined, respectively, as

$$\langle z^2 \rangle_{\mathrm{SOS}} = \sum_{p=0}^{\infty} \left[\sum_{q=0}^{\infty} A_{\mathrm{SOS}}(p,q) x^q \right] y^p , \tag{2.12}$$

$$\langle z^2 \rangle_{\mathrm{RSOS}} = \sum_{p=0}^{\infty} \left[\sum_{q=0}^{\infty} A_{\mathrm{RSOS}}(p,q) x^q \right] y^p . \tag{2.13}$$

The polynomials may be found in the Appendix, Eqs. (A3) and (A4). The singular behavior of the series is analyzed in the next section.

C. Numerical results for the roughening transition

We begin by recalling the bulk phase diagram in Fig. 1 as obtained from mean-field, Monte Carlo, low-

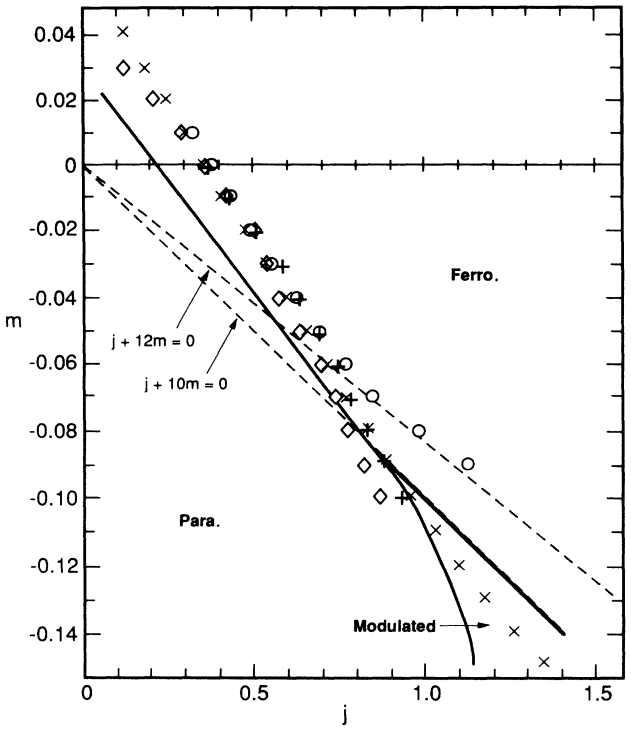

FIG. 1. Roughening transition lines based on $\langle z^2\rangle_{BO}$ denoted by ○, $\langle z^2\rangle_{SOS}$ denoted by × $\langle z^2\rangle_{RSOS}$ denoted by ◇, and $\mathcal{R}'_{BO}$ denoted by +. They are compared with the bulk phase boundaries (solid) quoted from Ref. 8.

temperature expansion, and ϵ-expansion methods, so that comparisons may be made with surface phase diagram. As shown in Fig. 1, the paramagnetic, ferromagnetic, and modulated phases merge at that point which we have labeled $\mathcal{L}$ ($j\sim -0.08$, $m\sim -0.9$). The boundary of the ferromagnetic-modulated phases is asymptotic to $j+10m=0$ in the $T\to 0$ limit.

Now we present the numerical results for the roughening transition obtained from the series, Eqs. (2.4), (2.5), (2.12), and (2.13). In Fig. 1 we plot the roughening transition lines obtained from $y_R(x)$ in Eq. (2.6). Near $m=0$, which is the Ising limit, all singular points from the different series are consistent with each other. Even for large $|m|$, all transition lines are almost consistent, except the line obtained from $\langle z^2\rangle_{BO}$. We interpret this discrepancy as follows. As $|m|$ increases, the bulk modulated phase becomes more favorable. Accordingly, bulk excitations cause modulated phase structure to develop parallel to the surface. A similar phenomenon was observed in earlier mean-field calculations.[7] This effect may enhance the contributions of bulk excitations in the series, Eq. (2.4), causing an apparent enhancement in the height fluctuations of the interface. At the moment, since we are interested in the evolution of the equilibrium interface fluctuations with increasing temperature, the order parameter $\langle z^2\rangle_{BO}$ is not appropriate to our study. Instead, we compute, the SOS model order parameter $\langle z^2\rangle_{SOS}$. We note that the transition lines obtained from the series, $\langle z^2\rangle_{SOS}$ and $\mathcal{R}'_{BO}$, are in good agreement, and this confirms the conjecture that the surface phase transition is not well described by calculations that are low order in $\langle z^2\rangle_{BO}$.

As one may see in Fig. 1, the roughening transition occurs at lower temperature than the para-ferromagnetic transition. However, as the effects of the competition in interactions become stronger, the roughening transition line becomes closer to the para-ferromagnetic transition line. Indeed, it seems likely that the roughening transition curve passes through the region where the bulk ferromagnetic, paramagnetic, and modulated phases are in close proximity. We return to this point later on in Sec. VI. On the other hand, for $m\lesssim -0.11$, the roughening transition line for the SOS model appears to be parallel to the bulk ferro-modulated phase boundary which, at low temperature, is asymptotic to $j+10m=0$. This suggests that modulated structure, rather like the bulk structure is forming at the interface. Indeed at $T=0$, for $j+10m=0\le 0$, the column layer structure with infinite height is more favorable than the flat surface. Moreover as in the bulk phase diagram, the equation $j+10m=0$ represents a degenerate line of multistate points at $T=0$. Thus, as in the bulk case, there is a progression of surface reconstructed phases. However, for the SOS model this is not so interesting, because the surface is at this stage already rough. Therefore the roughening transition line is $j+10m=0$ as $T\to 0$.

Now, the presence of the column modulated structure for $m\lesssim -0.11$ implies that the surface has large fluctuations with short-ranged correlation. In this case, the bending energy is more dominant than the microscopic surface tension. On the other hand, in the Ising model, $m\to 0$, it is known that the surface tension plays a dominant role in the formation of a rough surface with long-ranged correlation. Therefore we can expect some crossover behavior to occur between $-0.11<m<0$ from the surface tension dominant regime with a large correlation length to the bending-energy dominant regime with short correlation length. This crossover behavior is evidenced in the exponent θ. Thus θ increases for $m\gtrsim -0.06$, but decreases for $m\lesssim -0.06$ in Table I. Note that a smaller θ implies a shorter correlation length.

In order to further discuss this crossover behavior, we consider the Hamiltonian Eq. (2.8) in momentum space. We perform the Fourier transformation for the height variables,

$$h_j=\frac{1}{\sqrt{N}}\sum_q h_q e^{-iq\cdot j}\,, \tag{2.14}$$

and then write the Hamiltonian as

$$\frac{\mathcal{H}_{SOS}(q)}{kT}=\sum_q [4(j+4m)(2-\cos q_x-\cos q_y) +16m(1-\cos q_x\cos q_y) +4m(2-\cos 2q_x-\cos 2q_y)]h_q h_{-q}\,. \tag{2.15}$$

In the $q\to 0$ limit, Eq. (2.15) becomes

TABLE I. The values of θ as a function of m based on the SOS model.

m	θ
0.00	1.076
−0.02	1.154
−0.04	1.208
−0.06	1.239
−0.08	1.225
−0.10	1.138
−0.12	0.980
−0.14	0.794

$$\frac{\mathcal{H}_{\mathrm{SOS}}(q)}{kT}=\sum_{\mathbf{q}}[2(j+12m)q^2-8mq^4-\tfrac{4}{3}m(q_x^4+q_y^4)]\times h_{\mathbf{q}}h_{-\mathbf{q}}\ . \tag{2.16}$$

Here the coefficient of the first term plays the role of a surface tension, and that of the second term plays that of a bending energy. The last term turns out to be irrelevant. For $j+12m<0$, the surface tension term is negative. This implies that long-range correlation is no longer present. However, the bending energy is positive for $m<0$. This fact is related to the presence of the modulated phase, where the correlation length is short. Therefore the crossover behavior is expected to occur near the intersection to $j+12m=0$, which is estimated as $m\sim-0.06$. That is comparable to the crossover behavior for θ in Table I.

It is worth pointing out that the column modulated surface structure does not appear within the RSOS model. The reason is that the infinite height changes between NN columns are excluded. Moreover the crossover behavior occurs near the intersection to $j+8m=0$ instead of $j+12m=0$. That is due to the difference in the NN coupling constant. This effect may cause small discrepancies in the roughening transition lines of the SOS model and the RSOS model for large $|m|$ in Fig. 1. Finally, we note that this appears to be no theoretical description for the evolution from the surface-tension to bending-energy dominant regions, a matter to which we return in Sec. V.

III. PREROUGHENING TRANSITION

A. Preroughening transition

Recently another surface transition, the preroughening transition (PR), was introduced by den Nijs.[16] The PR transition is a transition from a flat surface to a disordered flat surface in which an array of steps with positional disorder and long-range up-down-up-down order exists. The original Hamiltonian that was used to study the PR transition is based on the RSOS-type model. It is the same as Eq. (2.11) except for the LNNN coupling. Therefore it is likely that this transition would also be present with the present Hamiltonian. Indeed one hopes to provide a confirmation of the existence of the PR transition line by the use of low-temperature expansions.

Let us begin this section by recalling the order parameter for the PR transition. The order parameter used in the original paper is $\langle\cos(\pi h)\rangle_{\mathrm{RSOS}}$ where h is a column height, and the brackets mean the average over the positions r. This quantity is finite in the ordered flat phase, and is zero in the disordered flat phase. However, we have obtained the low-temperature series for a slightly modified quantity,

$$N_{\mathrm{PR,RSOS}}\equiv 1-\langle\cos(\pi h)\rangle_{\mathrm{RSOS}}\ . \tag{3.1}$$

This form is more convenient because it causes the contribution of the flat surface at $T=0$ to be zero. The detailed polynomials appear in the Appendix, Eq. (A6). With the quantity (3.1), the PR transition line is determined as a curve of roots of $N_{\mathrm{PR,RSOS}}=1$. The solutions are located by the Newton method, and we have presented the results of the PR line in Fig. 2. In the same figure we also compare the roughening transition line and the PR transition line within the RSOS model. Note that they overlap in the region $j>0$, $m<0$, but are distinct in the region $j>0$, $m>0$. This diagram is topologically similar to Fig. 2 of Ref. 16.

We also examine the PR transition line with the SOS model $\langle\cos(\pi h)\rangle_{\mathrm{SOS}}$. The series may be found in the Appendix, Eq. (A5). We recall that there is no restriction in the column height change in the SOS model. In this case we could resolve the PR transition line from the roughening transition line even in the region $j>0$ and $m>0$. Consequently, we might conjecture that the PR transition is a characteristic of the RSOS model, not of the SOS model. Its significance for the true surface would, in this case, not be entirely clear. Evidently this problem will require further careful examination.

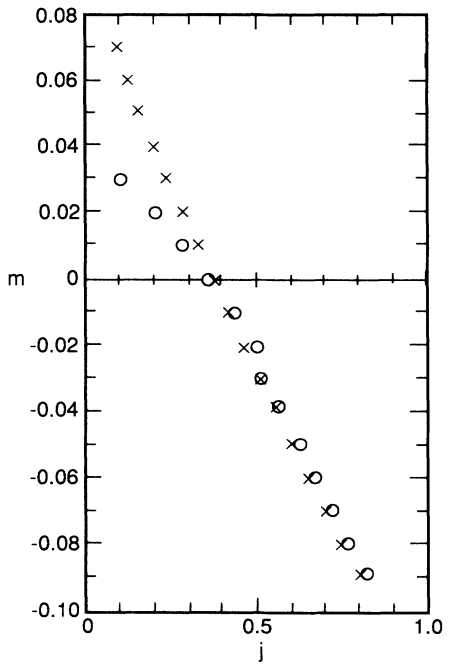

FIG. 2. Compared are the PR transition line × with the roughening transition line ○ based on the RSOS model.

B. Reconstructed surface structures

One of the features of the RSOS model with the competing interactions is the presence of the reconstructed surface structure. Thus by reconstructed surface structure we mean the flat rippled structure that is present, even at $T=0$. Interestingly this reconstructed structure grows from a multistate point as is the case for the bulk phase diagram.

We first consider a surface lamellar structure as shown in Fig. 3. In order to describe the configuration, we introduce a quantity l_s. Here s is the number of layers comprised of overtuned spins, and l is the height of the layers. A sequence of layer structures[10] is described by using the notation $\langle\ \rangle$. For example, the flat surface in the ferromagnetic phase is given by $\langle 0_\infty \rangle$. The configuration of Fig. 3 is denoted $\langle 1_2,0_2 \rangle$, the latter meaning a sequence of two layers with height one, and two layers with height zero. The $\langle 1_2,0_2 \rangle$ state corresponds to a two-band structure in the bulk phase, which is degenerated with the flat surface $\langle 0_\infty \rangle$ along $J+6M=0$ at $T=0$. When $J+6M<(>)0$, the phase $\langle 1_2,0_2 \rangle$ is more (less) favorable than the flat phase at $T=0$. However, since surface states include up-down symmetry with respect to the flat interface, the $\langle 1_2,0_2 \rangle$ state is infinitely degenerate with a linear combination of $\langle 1_2,0_2 \rangle$ and $\langle -1_2,0_2 \rangle$. For example, $\langle 1_2,0_2,-1_2,0_2 \rangle$ is one of the states.

Besides the degeneracy due to the up-down symmetry, the $\langle 1_2,0_2 \rangle$ state is also degenerate with $\langle 1_m,0_m \rangle$ for $m \geq 3$ when $J+6M=0$ at $T=0$. This degenerate behavior is analogous to the multistate point of k bands for $k \geq 2$ in the bulk case when $J+10M=0$ at $T=0$. In order to discuss the multiphase behavior of the surface, we rewrite $\langle 1_2,0_2 \rangle$ as $\langle 2 \rangle_S$, while two-band structure in the bulk is denoted as $\langle 2 \rangle_B$. The subscripts S and B stand for surface and bulk, respectively.

In the bulk phase, by calculating the one spin-flip excitation, it is known that $\langle k \rangle_B$ for $k \geq 4$ states are excluded when $T \neq 0$. Moreover near $T \sim 0$, the degeneracy of $\langle 2 \rangle_B$ and $\langle 3 \rangle_B$ is resolved by generating the states of $\langle 2^{k-1}3 \rangle_B$ for $k \geq 1$. Likewise, even in the surface phase, near $T \sim 0$, the states of $\langle 2^{k-1}3 \rangle_S$ for $k \geq 1$ are created. Thus the point of $J+6M=0$ at $T=0$ is a multiphase degenerate point at which $\langle 2 \rangle_S \sim \langle 3 \rangle_S$ phases are degenerate. Moreover for $J+6M \leq 0$, many multiphase points exist at $T=0$, which are tabulated in Table II.

TABLE II. The reconstructed surface structures at $T=0$. Here m is any integer for ≥ 2.

Configuration	Degenerate line
$\langle 1_m,0_m \rangle$	$J+6M=0$
$\langle 1_m,0_m,-1,0 \rangle$	$J+\frac{11}{2}M=0$
$\langle 1,0_m \rangle$ and $\langle 1,0,-1,0 \rangle$	$J+5M=0$
$\langle 1_m,0,1,0 \rangle$	$J+\frac{9}{2}M=0$
$\langle (1,0)_m,-1,0 \rangle$	$J+[4+2/(m+1)]M=0$
$\langle 1,0 \rangle$	$J+4M=0$

IV. ORIENTATIONAL ROUGHENING TRANSITION

A pinned, tensionless surface is believed to undergo two types of transition.[17–20] As the temperature is increased the interface undergoes a conventional scalar Coulomb-gas roughening (TR) transition at which the fluctuations in the height diverge. There remains some orientational order that is lost after one further Kosterlitz-Thouless (vector Coulomb-gas) transition. The latter is known as the orientational roughening (OR) transition. The OR transition results from the decorrelation of the surface normals to the interface,[20] while the TR transition is due to the increase in height-height fluctuations. Nelson and Halperin[17,18] considered the Laplacian roughening model and argued the presence of both the OR and TR transitions. Later numerical studies[19] for the Laplacian roughening model were performed, and evidence for two transitions was found, though they occur at very nearly the same temperature.

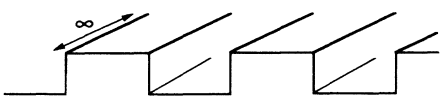

FIG. 3. A configuration of the reconstructed structures is shown.

A convenient order parameter for the OR transition is

$$N_{\mathrm{OR,SOS}} \equiv \left\langle \left[\sum_{j=1}^{4} (-1)^j h(r+\delta_j) \right]^2 \right\rangle_{\mathrm{SOS}} , \tag{4.1}$$

where $r+\delta_j$ is a NN site to r, and the brackets mean the average over the position r. We have obtained the low-temperature series for this order parameter and it is presented in the Appendix, Eqs. (A7) and (A8). As before, by using the d log Padé analysis, one can now locate the OR transition line. It is plotted in Fig. 4 along with the TR transition. Evidently the two lines are barely resolved for $m \gtrsim -0.06$, where the surface tension is moderately large. However, the two lines do not slightly deviate when $m < -0.1$, where the bending energy is supposed to be dominant, rather they are both parallel to the line $j+10m=0$. Hence it is not obvious that the OR transition line is distinct from the TR line. We attribute this result to the limited order of the low-temperature series.

V. DISCUSSIONS AND CONCLUSIONS

A. The sine-Gordon RG analysis

Most of the roughening transitions mentioned in the preceding sections may be studied using a sine-Gordon renormalization-group analysis. The translational roughening and preroughening transitions may be described using the Hamiltonian

$$\mathcal{H} = -\frac{\sigma}{2} \int d^2x (\nabla\phi)^2 + y_1 \int d^2x \cos 2\pi\phi + y_2 \int d^2x \cos 4\pi\phi \ . \tag{5.1}$$

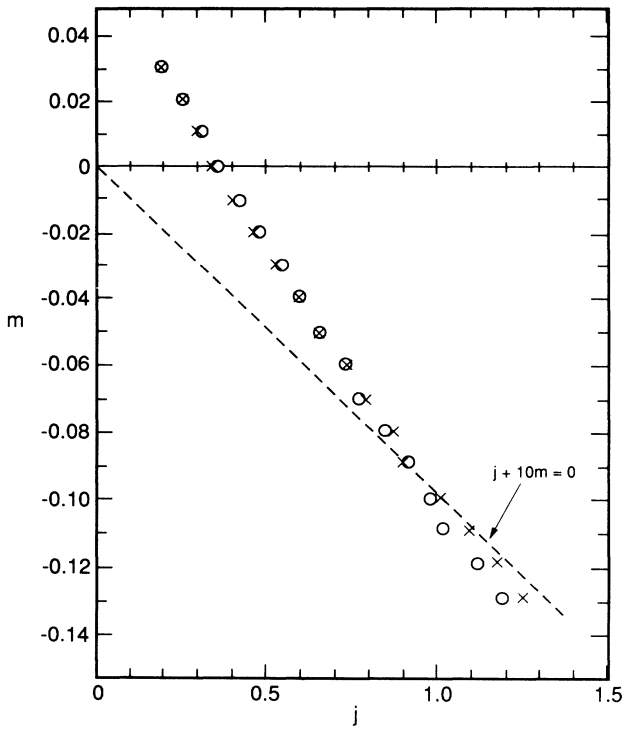

FIG. 4. The OR transition line × is compared with the roughening transition line ○ based on the SOS model.

The essential features of the analysis may be readily understood by examination of Fig. 5. Thus, depending on the choice of initial condition on the critical surface, one finds that two, one, or none of the fugacities flow to zero. If both do so, then one has no restraining potential for the surface, and it becomes rough. Conversely, if only one of the fugacities is finite, then the phase is prerough. Note that, when the coefficients of the cosines become finite, one often says that the charges that define their fugacities "unbind." Implicit is the basic relationship between the interfacial and the Coulomb-gas analysis.

Clearly the sine-Gordon analysis starting from Eq. (5.1) is straightforward. However, the claim that this effective Hamiltonian, Eq. (5.1), is equivalent to the basic lattice model is not firmly established, a matter to which we shall return in Sec. V B.

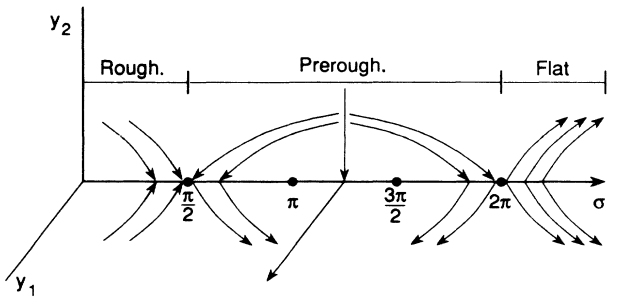

FIG. 5. RG flow diagram of the roughening and preroughening transitions.

The orientation roughening transition may also be formulated as a sine-Gordon renormalization-group problem.[20] The Hamiltonian has been determined to be

$$\mathcal{H}=-\frac{\kappa}{2}\int d^2x(\nabla^2\phi)^2+\lambda\sum_{\hat{a}}\int d^2x\,\cos\hat{a}\cdot\nabla\phi \qquad (5.2)$$

where $\hat{a}$ stands for the unit lattice vectors, and this Hamiltonian reproduces the flow equations for a vector Coulomb gas.[17,18] It transpires that there exists also an orientational preroughening transition by analogy with that for translational roughening,[20] though the structure of the phase diagram is somewhat richer for the orientational problem.

Combing the Hamiltonians (5.1) and (5.2) and adding a coupling term of the form

$$v\sum_{\hat{a}}\int d^2x\,\cos\alpha\phi\,\cos\hat{a}\cdot\nabla\phi \qquad (5,3)$$

with the coupling constant v, one may obtain both the translational and orientational roughening transitions from a single Hamiltonian, by appropriate choice of initial conditions on the initial surface. However, the interfacial phase diagram in the space of σ and κ has not yet been determined in that region where the orientational and translational transition collapse to a single translational roughening transition. There appears to be a rather spherical transition point located in this region. Further analysis of this problem will be presented at a later date.

B. Discussions and conclusions

As we pointed out in the Introduction to this paper, the nature of surface phase transitions in the Hamiltonian with extended interactions is still relatively poorly understood. Some of the results presented in this paper are inconclusive and must be viewed as a first step in systematic investigation of the problem. A curve of TR transitions was clearly identified and the exponent θ was calculated. The origin of the variation of the exponent along the roughening curve is not properly understood. Possibly it is a consequence of the limited order of the low-temperature series, but given the size of the variation compared with the typical errors, one might question this conclusion. It is also possible that one is observing crossover due to proximity of the vector Coulomb-gas fixed point, but since the series is unable to resolve this transition, there is no simple way of checking this conjecture.

The presence of the PR transition within the RSOS model is encouraging in that it appears to confirm the predictions of den Nijs. However, the PR transition could not be observed for the Ising or the SOS model, and one is concerned that the phenomenon might be present only in the restricted model. Presumably this would mean that the transition is unlikely to be observed in real surfaces. The sine-Gordon renormalization arguments of den Nijs are based on the ideal that $\pm 2e$ charges of $\cos 4\pi\phi(x)$ can unbind at higher (Coulomb-gas) temperature than the $\pm e$ charges of $\cos 2\pi\phi(x)$. The vanishing of the fugacity of the $\cos 2\pi\phi(x)$ term results in a

Kosterlitz-Thouless transition that is universal and has a fixed exponent. The unbinding of the $\pm 2e$ charges should result in a PR transition. However, this transition is no longer universal because the fugacity of the first harmonic is still finite and the interface height-height correlations are still suppressed. This results in a continuously varying exponent along the putative PR line. Given the nature of the transition, it is possible that, for an SOS model, there exists a more relevant operator than the $\cos 4\pi\phi(x)$ term, and this may ultimately preclude the PR transition. It is known that the $\cos 2\pi\phi(x)$ operator is more relevant than any other, so the true roughening transition would not be affected by such effects.

Another alternative explanation is as follows. Within the sine-Gordon formulation one may choose initial conditions for the surface free energies and the coefficients of the harmonic operators corresponding, in the Coloumb-gas language, to the fugacities of the charges. In the microscopic Hamiltonian one chooses only the surface free-energy terms. Consequently, a given RSOS or SOS model Hamiltonian must imply some fixed choice for the bare initial conditions. It is possible that the SOS model implies initial conditions that do not permit a flow to the PR region. The fact that the microscopic RSOS model significantly enhances those configurations that drive the PR transition may reflect this behavior.

Finally our observation might also be rationalized as follows. We have noted that the RSOS restrictions enhance those configurations that drive the PR transition. Thus it may be that the transition is present in both SOS and RSOS theories but that the low-temperature expansion is only capable of capturing it when it is perspicuous, that is, within the RSOS model. Evidently, these issues will have to be investigated further.

The lack of evidence for an OR transition from the low-temperature expansion is, perhaps, not so surprising. The PR transition is driven by configurations that are well represented at low order in the series. The OR transition results from decreasing correlation of coarse-grained surface normals. The order of the present series permits only rather compact excitations and this may not be sufficient to define significantly separated, oriented normals. Thus the orientation of the surface, as described by the expansion, becomes decorrelated only whenever the height fluctuations diverge; that is, whenever the conventional TR roughening transition takes place. This reasoning is consistent with our observation that the curves of OR and TR transitions, as signaled by their respective order parameters, are essentially degenerate. We have undertaken the task of obtaining the low-temperature series to higher order and, though this may well resolve the preroughening issue, it does not seem likely that this will be sufficient to resolve the question of the OR transition. Thus for the moment we must rely on the conclusions of the sine-Gordon analysis discussed in the preceding section.

The question of surface reconstruction is also of some interest, and probably worth pursuing. The observation that, for our model, multiphase surface reconstruction is present, suggests that such a phenomenon may be present in nature. However, the detailed evolution of the phase diagram in this region is not yet understood. Evidently, there are two prominent tendencies. Thus the surface ripples can melt and if this is described by some defect Hamiltonian, one would ultimately be led to a floating phase akin to that of the two-dimensional ANNNI model. However, the surface is still free to undergo overall height fluctuations. If these become unbounded before the melting of the ripples one presumes that the roughening transition is merely shifted in temperature. However, if these fluctuations compete, then the surface free energies will be renormalized by both height fluctuations and the meandering of the surface ripples. This problem is presently under study.

At this stage it is, perhaps, worth placing some of the observations of this paper in the broader context of the bulk phase diagram. As we mentioned in the Introduction, one of the fundamental objectives of the study was the hope that some light would be cast on that region of the bulk phase diagram where the ferromagnetic, and modulated phases were in close proximity. Within mean-field theory, these three phases merge at an isotropic Lifshitz point $\mathcal{L}$ at which the period of the modulated phase diverges.

However, fluctuations strongly renormalize the paramagnetic-modulated boundary and drive it to fluctuation-induced first order. Furthermore, based on naive engineering dimensions, the lower critical dimension of the isotropic Lifshitz point $\mathcal{L}$ is $d_L = 4$. For these reasons, it seems unlikely that mean-field theory can be relied upon in this region of the phase diagram. On the other hand, Monte Carlo simulations of this region are inconclusive as to the nature of the Lifshitz point, though they do provide a fairly reliable guide to the location of the transitions. We argue that, if the mean-field prediction that the period of the lamellar diverges at the transition is valid, then the bulk order-disorder transition may be connected to the roughening of dilute interacting layers. In fact, it is noted that, within numerical error, the roughening curve from low-temperature expansions passes through the putative point $\mathcal{L}$ as calculated by simulation. This is hardly compelling evidence that the two phenomena are related but it has prompted us to begin to study the collective roughening of tensionless surfaces.

Though the low-temperature expansion was unable to locate the translationally rough, oriented interface, it is probably present for the Hamiltonians, Eqs. (5.1) and (5.2). If this is indeed the case, and the lamellae in the bulk phase are indeed far apart in the vicinity of $\mathcal{L}$, one has the intriguing possibility that a second bulk orientationally disordered phase may exist. Presumably this phase would be composed of dilute interfaces each of which is orientationally smooth, but transitionally rough.

Evidently, for both the bulk and surface Hamiltonians there is much yet to be done, and it seems possible that some qualitatively novel phenomena may emerge from the study.

ACKNOWLEDGMENTS

We have benefited from conversations with Y. Levin and Professor J. D. Weeks. One of us (K.A.D.) gratefully

acknowledges support from the Sloan Foundation. A. B. thanks the NSF for financial support. B. K. acknowledges support from the Regents of the University of California.

APPENDIX

The polynomials are presented below with $x \equiv e^{-4M/kT}$ and $y \equiv e^{-4J/kT}$.

The series for $\langle z^2 \rangle_{\mathrm{BO}}$ is

$$\begin{aligned}\langle z^2\rangle_{\mathrm{BO}} = {} & y^2(2x^6)+y^3(8x^{12}+6x^{14}-8x^{15})+y^4(8x^{10}+8x^{11}-36x^{12}+8x^{14}+24x^{16}+12x^{17}+16x^{20}) \\ & +y^5(2x^{12}+48x^{16}+72x^{17}-280x^{18}+32x^{19}+68x^{20}+60x^{21} \\ & \quad +16x^{22}+80x^{23}+40x^{24}+24x^{26}+24x^{28}+16x^{29}-58x^{30}) \\ & +y^6(24x^{13}+12x^{14}+48x^{15}-276x^{16}-360x^{17}+848x^{18}+136x^{19}-158x^{20}+268x^{21}-784x^{22} \\ & \quad -352x^{23}+80x^{24}+368x^{25}-108x^{26}+268x^{27}+162x^{28}+100x^{29}+394x^{30} \\ & \quad +106x^{32}+18x^{34}+32x^{36}) \\ & +y^7(24x^{16}+24x^{17}-78x^{18}+160x^{19}+168x^{20}+596x^{21}-2592x^{22}-4568x^{23}+10\,848x^{24}+236x^{25} \\ & \quad -3260x^{26}-758x^{27}-1736x^{28}-3528x^{29}+1072x^{30}+3456x^{31}-1136x^{32}+2152x^{33}+762x^{34} \\ & \quad +524x^{35}+624x^{36}+312x^{38}+72x^{39}+152x^{40}+124x^{41}+104x^{42}-378x^{43}-106x^{44}) . \end{aligned} \tag{A1}$$

The series for $[\rho(\frac{1}{2})+\rho(\frac{3}{2})]_{\mathrm{BO}}$ is

$$\begin{aligned}[\rho(\tfrac{1}{2})+\rho(\tfrac{3}{2})]_{\mathrm{BO}} = {} & y^2(x^6)+y^3(4x^{12}+x^{14})+y^4(4x^{10}+4x^{11}-18x^{12}+4x^{14}+12x^{16}+6x^{17}+6x^{20}) \\ & +y^5(x^{12}+24x^{16}+36x^{17}-164x^{18}+16x^{19}+41x^{20}+33x^{21} \\ & \quad +8x^{22}+40x^{23}+12x^{24}+12x^{26}+4x^{28}+x^{29}) \\ & +y^6(12x^{13}+6x^{14}+24x^{15}-154x^{16}-198x^{17}+424x^{18}+68x^{19}-79x^{20}+134x^{21} \\ & \quad -432x^{22}-198x^{23}+8x^{24}+176x^{25}-27x^{26}+106x^{27}+142x^{28}+122x^{29} \\ & \quad +52x^{30}+37x^{32}+2x^{34}+8x^{36}) \\ & +y^7(12x^{16}+12x^{17}-39x^{18}+80x^{19}+76x^{20}+294x^{21}-1400x^{22}-2452x^{23}+5572x^{24} \\ & \quad +110x^{25}-1842x^{26}-555x^{27}-956x^{28}-1936x^{29}+736x^{30}+1700x^{31} \\ & \quad -630x^{32}+924x^{33}+521x^{34}+277x^{35}+293x^{36}+96x^{38}+20x^{39}+36x^{40}+14x^{41}+4x^{42}+x^{43}) . \end{aligned} \tag{A2}$$

The series for $\langle z^2 \rangle_{\mathrm{SOS}}$ is

$$\begin{aligned}\langle z^2\rangle_{\mathrm{SOS}} = {} & y^2(2x^6)+y^3(8x^{12})+y^4(8x^{10}+8x^{11}-36x^{12}+8x^{14}+24x^{16}+12x^{17}+16x^{20}) \\ & +y^5(48x^{16}+72x^{17}-312x^{18}+32x^{19}+104x^{20}+64x^{21}+16x^{22}+80x^{23}+40x^{24}+24x^{26}) \\ & +y^6(24x^{13}+12x^{14}+48x^{15}-276x^{16}-360x^{17}+848x^{18}+136x^{19}-182x^{20}+268x^{21} \\ & \quad -784x^{22}-352x^{23}-40x^{24}+368x^{25}+12x^{26}+196x^{27}+336x^{28}+272x^{29} \\ & \quad +120x^{30}+50x^{32}+18x^{34}+32x^{36}) \\ & +y^7(160x^{19}+128x^{20}+576x^{21}-2672x^{22}-4688x^{23}+11\,648x^{24}+384x^{25}-4272x^{26} \\ & \quad -896x^{27}-1928x^{28}-3664x^{29}+1464x^{30}+3744x^{31}-1592x^{32}+1952x^{33} \\ & \quad +1296x^{34}+576x^{35}+528x^{36}+312x^{38}+72x^{39}+80x^{40}) . \end{aligned} \tag{A3}$$

The series for $\langle z^2 \rangle_{\mathrm{RSOS}}$ is

$$\begin{aligned}\langle z^2\rangle_{\mathrm{RSOS}} = {} & y^2(2x^6)+y^3(8x^{12})+y^4(8x^{10}+8x^{11}-36x^{12}+8x^{14}+24x^{16}+12x^{17}+8x^{20}) \\ & +y^5(48x^{16}+72x^{17}-312x^{18}+32x^{19}+104x^{20}+64x^{21}+16x^{22}+80x^{23}+24x^{26}) \\ & +y^6(24x^{13}+12x^{14}+48x^{15}-276x^{16}-360x^{17}+848x^{18}+136x^{19}-182x^{20}+268x^{21} \\ & \quad -784x^{22}-352x^{23}-80x^{24}+328x^{25}+144x^{26}+172x^{27}+220x^{28}+224x^{29}+64x^{30}+50x^{32}) \\ & +y^7(160x^{19}+128x^{20}+576x^{21}-2672x^{22}-4688x^{23}+11\,648x^{24}+384x^{25}-4272x^{26} \\ & \quad -952x^{27}-2120x^{28}-3952x^{29}+2504x^{30}+3080x^{31}-1280x^{32}+1344x^{33} \\ & \quad +1096x^{34}+448x^{35}+384x^{36}+88x^{38}) . \end{aligned} \tag{A4}$$

The series for $N_{\mathrm{PR,SOS}}$ is

$$\begin{aligned} N_{\mathrm{PR,SOS}} = {} & y^2(4x^6)+y^3(16x^{12})+y^4(16x^{10}+16x^{11}-52x^{12}+16x^{14}+48x^{16}+24x^{17}+16x^{20}) \\ & +y^5(96x^{16}+144x^{17}-520x^{18}+64x^{19}+208x^{20}+128x^{21}+32x^{22}+160x^{23}+48x^{26}) \\ & +y^6(48x^{13}+24x^{14}+96x^{15}-448x^{16}-600x^{17}+1696x^{18}+272x^{19}-260x^{20}+536x^{21} \\ & \quad -1320x^{22}-560x^{23}-144x^{24}+672x^{25}+356x^{26}+360x^{27}+512x^{28}+480x^{29}+176x^{30}+100x^{32}+4x^{34}) \\ & +y^7(320x^{19}+256x^{20}+1152x^{21}-4800x^{22}-8480x^{23}+23\,296x^{24}+1056x^{25}-7456x^{26} \\ & \quad -1136x^{27}-3944x^{28}-7008^{29}+4544x^{30}+6720x^{31}-2552x^{32}+3264x^{33}+2368x^{34} \\ & \quad +1024x^{35}+928x^{36}+240x^{38}+16x^{39}+32x^{40}) . \end{aligned} \tag{A5}$$

The series for $N_{\mathrm{PR,RSOS}}$ is

$$\begin{aligned} N_{\mathrm{PR,RSOS}} = {} & y^2(4x^6)+y^3(16x^{12})+y^4(16x^{10}+16x^{11}-72x^{12}+16x^{14}+48x^{16}+24x^{17}+16x^{20}) \\ & +y^5(96x^{16}+144xx^{17}-624x^{18}+64x^{19}+208x^{20}+128x^{21}+32x^{22}+160x^{23}+48x^{26}) \\ & +y^6(48x^{13}+24x^{14}+96x^{15}-552x^{16}-720x^{17}+1696x^{18}+272x^{19}+52x^{20}+536x^{21} \\ & \quad -1568x^{22}-704x^{23}-160x^{24}+656x^{25}+288x^{26}+344x^{27}+440x^{28}+448x^{29}+128x^{30}+100x^{32}) \\ & +y^7(320x^{19}+256x^{20}+1152x^{21}-5344x^{22}-9376x^{23}+23\,296x^{24}+768x^{25}-3744x^{26} \\ & \quad -1904x^{27}-4240x^{28}-7904x^{29}+5008x^{30}+6160x^{31}-2560x^{32}+2688x^{33} \\ & \quad +2192x^{34}+896x^{35}+768x^{36}+176x^{38}) . \end{aligned} \tag{A6}$$

The series for $N_{\mathrm{OR,SOS}}$ is

$$\begin{aligned} N_{\mathrm{OR,SOS}} = {} & y^2(8x^6)+y^3(32x^{12})+y^4(16x^{10}+40x^{11}-144x^{12}+32x^{14}+64x^{16}+56x^{17}+48x^{20}) \\ & +y^5(128x^{16}+336x^{17}-1248x^{18}+80x^{19}+400x^{20}+224x^{21}+80x^{22}+160x^{23}+160x^{24}+48x^{26}) \\ & +y^6(48x^{13}+16x^{14}+160x^{15}-640x^{16}-1680x^{17}+3328x^{18}+496x^{19}-976x^{20}+952x^{21} \\ & \quad -2064x^{22}-1704x^{23}-800x^{24}+1440x^{25}+192x^{26}+448x^{27}+944x^{28} \\ & \quad +672x^{29}+224x^{30}+96x^{32}+72x^{34}+128x^{36}) \\ & +y^7(400x^{19}+256x^{20}+2016x^{21}-7120x^{22}-21\,696x^{23}+45\,760x^{24}+3328x^{25}-17\,440x^{26} \\ & \quad -3400x^{27}-7824x^{28}-9664x^{29}+2288x^{30}+10\,944x^{31}-4456x^{32}+4464x^{33} \\ & \quad +3216x^{34}+1184x^{35}+1024x^{36}+928x^{38}+320x^{39}+192x^{40}) . \end{aligned} \tag{A7}$$

The series for $N_{\mathrm{OR,RSOS}}$ is

$$N_{O,SOS}=y^2(8x^6)+y^3(32x^{12})+y^4(16x^{10}+40x^{11}-144x^{12}+32x^{14}+64x^{16}+56x^{17}+16x^{20})$$
$$+y^5(128x^{16}+336x^{17}-1248x^{18}+80x^{19}+400x^{20}+224x^{21}+80x^{22}+160x^{23}+48x^{26})$$
$$+y^6(48x^{13}+16x^{14}+160x^{15}-640x^{16}-1680x^{17}+3328x^{18}+496x^{19}-976x^{20}+952x^{21}$$
$$-2064x^{22}-1784x^{23}+704x^{24}+1248x^{25}+752x^{26}+344x^{27}+608x^{28}+448x^{29}+96x^{30}+96x^{32})$$
$$+y^7(400x^{19}+256x^{20}+2016x^{21}-7120x^{22}-21\,696x^{23}+45\,760x^{24}+3328x^{25}$$
$$-17\,440x^{26}-4224x^{27}-8400x^{28}-11\,296x^{29}+6768x^{30}+8752x^{31}-3136x^{32}$$
$$+2832x^{33}+2480x^{34}+864x^{35}+672x^{36}+160x^{38})\ . \qquad \text{(A8)}$$

[1]Recent review is J. D. Weeks, in *Ordering in Strongly Fluctuating Condensed Matter Systems,* edited by T. Riste (Plenum, New York, 1980).

[2]J. D. Weeks, G. H. Gilmer, and H. J. Leamy, Phys. Rev. Lett. **31**, 549 (1973).

[3]S. T. Chui and J. D. Weeks, Phys. Rev. B **14**, 4978 (1976).

[4]B. Widom, J. Chem. Phys. **84**, 6943 (1986).

[5]K. A. Dawson, M. D. Lipkin, and B. Widom, J. Chem. Phys. **88**, 5149 (1988).

[6]K. A. Dawson, Phys. Rev. A **35**, 1766 (1987).

[7]K. A. Dawson, Phys. Rev. A **36**, 3383 (1987).

[8]K. A. Dawson, B. Walker, and A. Berera, Physica A **165**, 320 1990.

[9]P. J. Upton and J. M. Yeomans, Europhys. Lett. **5**, 575 (1988); Phys. Rev. B **40**, 439 (1989).

[10]M. E. Fisher and W. Selke, Phys. Rev. Lett. **44**, 1502 (1980); Philos. Trans. R. Soc. London **302**, 1 (1981).

[11]Y. Levin and K. A. Dawson, Phys. Rev. A **42**, 1976 (1990).

[12]M. C. Barbosa (unpublished).

[13]J. L. Martin, in *Phase Transitions and Critical Phenomena,* edited by C. Domb and M. S. Green (Academic, New York, 1972), Vol. 3; S. Redner, J. Stat. Phys. **29**, 309 (1982).

[14]B. Kahng (unpublished).

[15]T. Ohta and K. Kawasaki, Prog. Theor. Phys. **60**, 365 (1978).

[16]M. den Nijs, Phys. Rev. Lett. **64**, 435 (1990); K. Rommelse and M. den Nijs, *ibid.* **59**, 2578 (1987); Phys. Rev. B **40**, 4709 (1989).

[17]D. R. Nelson and B. I. Halperin, Phys. Rev. B **19**, 2457 (1979).

[18]A. P. Young, Phys. Rev. B **19**, 1855 (1979).

[19]K. J. Strandburg, S. A. Solla, and G. V. Chester, Phys. Rev. B **28**, 2717 (1983).

[20]Y. Levin and K. A. Dawson, Phys. Rev. A **42**, 3507 (1990).